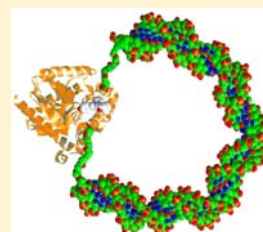


Mechanical Control of Renilla Luciferase

Chiao-Yu Tseng* and Giovanni Zocchi*

Department of Physics and Astronomy, University of California, Los Angeles, Los Angeles, California 90095-1547, United States

ABSTRACT: We report experiments where the activity of the enzyme luciferase from *Renilla reniformis* is controlled through a DNA spring attached to the enzyme. In the wake of previous work on kinases, these results establish that mechanical stress applied through the DNA springs is indeed a general method for the artificial control of enzymes, and for the quantitative study of mechano-chemical coupling in these molecules. We also show proof of concept of the luciferase construct as a sensitive molecular probe, detecting a specific DNA target sequence in an easy, one-step, homogeneous assay, as well as SNP detection without melting curve analysis.



INTRODUCTION

Mechanical control of enzymatic activity is in principle a universal method for modulating the speed of enzymes, potentially enabling the modular design of molecular control mechanisms and probes.¹ Proteins are deformable molecules,² and enzymes in particular undergo a cyclic deformation as they bind their substrates and release the products. An external mechanical stress on the enzyme will therefore in general perturb this cycle and lead to a modulation of activity.³ In practice, DNA molecular springs^{3–5} have been used to exert nondestructive mechanical stresses on an enzyme, leading to a modulation of activity.^{1,3–7} MD simulations can provide insight into the atomistic or microscopic basis of this mechano-chemical coupling,⁸ but quantitatively relating changes in enzymatic rate to the force on the enzyme is challenging. On the other hand, the question of the role and distribution of the elastic energy in cooperative allosteric transitions has a long history^{9,10} while mechano-sensitive enzymes is a topic of current research interest.^{11–14}

Our method consists of synthesizing an enzyme–DNA chimera where a single-stranded DNA oligomer (typically 60 bases long and thus very flexible: the persistence length of ss DNA corresponds to approximately 3 bases, while for ds DNA it is approximately 150 bp) is covalently attached by the ends to two specific surface sites on the enzyme (labeled by Cys residues introduced by mutagenesis). Hybridization to the complementary strand rigidifies the DNA spring, which exerts a mechanical stress on the enzyme. Most of the work to date has been performed with the enzyme guanylate kinase (GK) although the method was originally demonstrated with the maltose binding protein (MBP);³ in particular, we showed how a spring pulling along the direction of the “hinge motion” of GK^{15,16} modulates the enzymatic activity,¹⁷ and we also found that different pulling directions can affect different specific parameters of the enzymatic cycle.¹⁸ Here we report the mechanical control of a different enzyme, Renilla luciferase (RLuc). The overall structure of this enzyme (Figure 1) is quite different from the structure of GK (and MBP): there is no “hinge” or hinge motion, and it is not a nucleotide binding protein. Our observation that we can modulate the activity of

this enzyme with the same mechanical method vindicates the view that the method is general. In addition, the RLuc–DNA chimera turns out to be a remarkably clean system where the nonstress-specific effects which are sometimes observed with GK¹⁹ are either absent or very small. The detection of enzymatic activity is convenient, with relatively high sensitivity, as the reaction produces visible light. These features make the luciferase–DNA chimera an interesting model system both to study the effect of mechanical stress on enzyme functioning, i.e. mechano-chemical coupling, and for biotechnology as a molecular probe. As a proof of concept of the latter, we report detection of femtomoles of specific DNA oligonucleotides in an easy homogeneous assay, as well as SNP detection without melting curve analysis.

RESULTS

Luciferase from *R. reniformis* (RLuc) is a 36 kD enzyme which catalyzes the oxidation of luciferin coelenterazine by molecular oxygen, producing coelenteramide, CO₂ and light (470 nm), with a rather low quantum yield of 5%.^{20,21} The Michaelis–Menten constant of the Coelenterazine-h (a modified substrate we use) is 220 nM.²⁰ Although irrelevant to this study, we mention that in *R. reniformis*, the bioluminescent process actually involves three components: RLuc, green fluorescent protein (RrGFP), and Ca²⁺-activated luciferin binding protein.²² In the presence of Ca²⁺, the luciferin binding protein releases luciferin, initiating catalysis by RLuc. The energy generated by this oxidation is transferred to RrGFP and then emitted as a green-wavelength photon. This process can presumably lead to a larger effective quantum yield, and indeed this is utilized in biotechnology.^{23,24}

In structural terms, RLuc consists of two domains, an α/β hydrolase domain and a cap domain; the latter contains a binding pocket for the substrate and is expected to be comparatively flexible.²⁵ At high concentrations (>1 mg/mL), RLuc slowly self-associates; this phenomenon does not involve disulfide bond formation of the internal cysteines.²⁶ The product

Received: May 1, 2013

Published: July 17, 2013

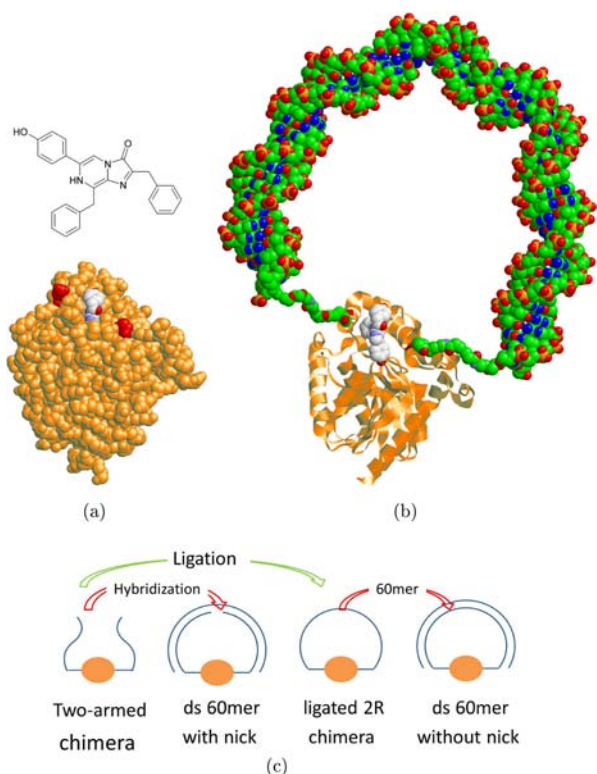


Figure 1. (a) Crystal structure of Renilla luciferase (colored light yellow) with bound substrate (coelenterazine) from Protein Data Bank (PDB) structure 2PSJ. Residues 161 and 188, mutated to cysteins in the experiment, are colored red. The distance between these two residues is $\sim 2\text{nm}$. (b) Cartoon of the RLuc–DNA chimera with the DNA spring attached to sites 161/188. The RLuc structure is from PDB 2PSJ and DNA is from the nucleosome structure 1KX5. The protein, DNA, and cross-linkers are drawn approximately to scale. (c) Sketch of the different forms of the RLuc chimera used in this study. The molecule is synthesized as a two-armed chimera (2R chimera), with two separate ss 30mer DNA strands coupled to the cross-linkers at the 5' and 3' end, respectively. Ligation of this construct results in the “ligated chimera”, sporting one continuous ss 60mer DNA strand attached by the ends to the cross-linkers. Hybridization of the ligated chimera to the complementary 60mer results in an enzyme under stress. Hybridization of the 2R chimera to the complementary 60mer results in an enzyme under a smaller stress because of the nick in the DNA spring.

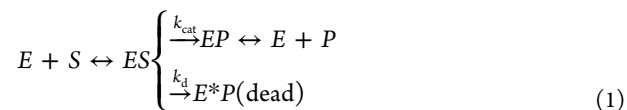
of the RLuc-catalyzed reaction is a strong competitive inhibitor of the enzyme ($K_i \approx 23\text{ nM}$).²⁶ Another feature of RLuc is that the enzyme inactivates after a relatively small number of catalytic cycles. The wild-type enzyme can catalyze about 100 reactions before inactivating.²⁷

We have introduced Cys residues at the locations 161 and 188 on RLuc, see Figure 1, and synthesized “two-armed” chimeras¹⁹ where two ss DNA 30mers are covalently attached to the Cys residues by the 3' and 5' ends, respectively (see Experimental Section). Hybridization with a complementary 60mer results in a DNA spring with a nick in the middle. Starting from the two-arms chimeras, we also synthesize a “ss chimera” by ligating the ends of the two DNA arms;¹⁹ hybridization with a complementary 60mer now results in a DNA spring without nick.

Mechanical control of luciferase activity is shown in Figure 2, where we report the time course of luminescence measurements under no stress (blue circles), a small stress (green

squares: nicked DNA spring), a larger stress (red triangles: ligated ds DNA spring). The mechanical stress exerted by the DNA spring in the ligated, ds form leads to partial inhibition of the enzyme. Figure 2c is a control where the two-armed chimera is hybridized with two separate 30mers (i.e., the DNA spring is disjoint so there is no stress), showing that the mere presence of DNA in close proximity to the enzyme does not affect the activity. Luciferase activity is often quantified by the integrated light intensity emitted over a time period (area under the curves of Figure 2); this measure is reported in Figure 2d.

In order to analyze the activity curves in more detail, we need a fit for the time-course measurements of Figure 2. These are actually not simple exponentials or sum of exponentials curves, and although the effects which produce this peculiar time course are known, we do not find corresponding fits in the literature. The main effects to be considered are product inhibition²⁶ and a stochastic process whereby the enzyme goes irreversibly into an inactive state after so many turnovers on average.²⁷ This “bleaching” is presumably related to the low quantum yield $Q \approx 5\%$ ^{20,21} of the photon-emitting reaction. Qualitatively, under conditions where the molar ratio of enzyme to substrate is small, the steep decrease in luminescence at the beginning of the time measurements (Figure 2) is due to the inactivation of the enzyme; gradually, inhibition by the accumulated products slows down the reaction, leading to the long tail in the graphs (Figures 2 and 3). Within a Michaelis–Menten description of the reaction speed:



where E is the enzyme, S the substrate, P the product, k_{cat} the catalytic rate, and k_d the inactivation rate of the enzyme, the rate of emitting photons is:

$$\frac{d}{dt}N_\gamma = \frac{[E]k_{\text{cat}}VQ}{1 + \frac{K_S}{[S]} + \frac{K_P[P]}{K_P[S]}} \quad (2)$$

where V is the reaction volume, Q the quantum yield, K_S and K_P the Michaelis–Menten constants of substrate and product, $[S]$ and $[P]$ the concentration of substrate and product, respectively, and $[E] = [E](t)$ is the total concentration of active enzymes at time t , governed by the rate equation:

$$\frac{d[E]}{dt} = -[ES]k_d = -\frac{[E]k_d}{1 + \frac{K_S}{[S]} + \frac{K_P[P]}{K_P[S]}} \quad (3)$$

$$\Rightarrow \frac{d[E]}{dt} = -\frac{dN_\gamma}{dt} \frac{1}{VQ} \frac{k_d}{k_{\text{cat}}} \quad (4)$$

To fit the time course measurements, we integrate the system of eqs 2 and 3) (see Experimental Section, keeping in mind that

$$\frac{d[S]}{dt} = -\frac{1}{VQ} \frac{dN_\gamma}{dt}, \quad \frac{d}{dt}[P] = -\frac{d}{dt}[S] \quad (5)$$

and adjust the parameters to reproduce the experimental curves. Some fits are shown in Figure 3, and the results are summarized in Table 1. In eq 4, k_{cat}/k_d represents the average turnover number of an enzyme before inactivation. Under stress, both k_d and k_{cat} increase by $\sim 30\%$, and the parameter B , which is proportional to the quantum yield Q (see

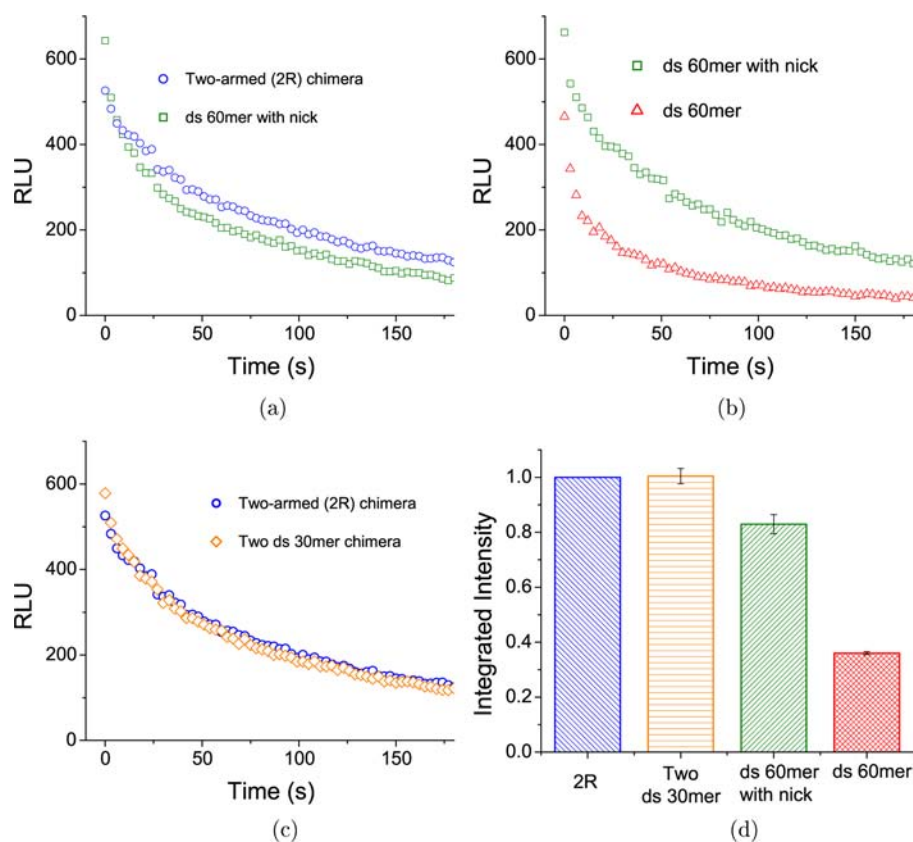


Figure 2. The time course of luminescence intensity (arbitrary units) for the RLuc chimera under different states of mechanical stress. The conditions are: 2 nM chimera concentration, 1 μ M initial substrate concentration. (a) Two-armed chimera (circles) and two-armed chimera hybridized to the complementary 60mer (ds with nick: squares). The DNA spring with the nick has only a small effect on the speed of the enzyme. (b) Ligated chimera hybridized with two complementary 30mers (DNA RA and RB: ds with nick: squares) and ligated two-armed chimera hybridized to the 60mer (ds without nick: triangles). The DNA spring without nick has a larger effect on the speed of the enzyme. (c) Two-armed chimera (circles) and two-armed chimera hybridized with two separate complementary 30mers (DNA RA and RB: two ds 30mer: diamonds). This is a control which shows that, merely bringing DNA in close proximity to the enzyme, without stress, has no effect on the enzymatic activity. (d) Integrated luminescence intensity (area under the curves in (a), (b), and (c) from $t = 0$ to $t = 120$ s) for the two-armed chimera (no stress), the chimera with two separately hybridized arms (control with no stress), the ds chimera with nick (small stress), and the ds chimera without nick (larger stress), normalized by the result of the two-armed chimera. The error bars are generated from three measurements for each construction.

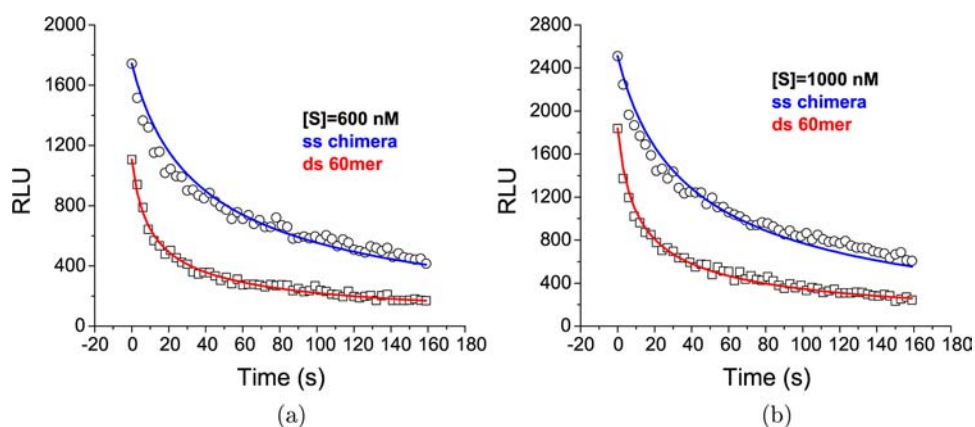


Figure 3. Experimental data (dots) and fits (lines) of the luminescence intensity vs time. (a) Time course of luminescence intensity for the unhybridized chimera (no stress: circles) and ds chimera (stressed: squares) with initial substrate concentration of 600 nM. (b) Initial substrate concentration = 1000 nM. The somewhat complicated fit is explained in the Experimental Section, and the parameters extracted from it are reported in Table 1.

Experimental Section), is reduced by $\sim 25\%$, so that the average turnover number before inactivation is essentially unaffected by the stress, while the quantum yield is lower. Further, K_S is doubled, while K_P is reduced by a factor 4. These parameter

changes are reflected in the change of shape of the time course curves (Figures 2 and 3) under mechanical stress: the increase in the rates k_d and k_{cat} causes the curve to be steeper at short times, while the decrease in K_P (stronger product inhibition)

Table 1. Kinetic Parameters Obtained from Fitting the Time Course Measurements As in Figure 3, for the ss (no stress) and ds (stressed) Chimera^a

	substrate conc. (nM)	ss chimera $K_S = 1.2 \pm 0.2 \times 10^3$ (nM)	ds 60mer chimera $K_S = 2.4 \pm 0.5 \times 10^3$ (nM)
k_d (1/s)	600	1.8×10^{-2}	2.4×10^{-2}
	750	1.5×10^{-2}	2.5×10^{-2}
	1000	1.6×10^{-2}	2.5×10^{-2}
K_p (nM)	600	17	4.3
	750	20	4.0
	1000	19	5.9
k_{cat} (1/s)	600	1.3	1.8
	750	1.3	1.7
	1000	1.2	1.9
B	600	1.6	1.2
	750	1.6	1.3
	1000	1.8	1.3

^aResults for three different initial substrate concentrations are reported. Since the values of the kinetic parameters are, in principle, independent of initial substrate concentration, the corresponding variations in the table are a measure of the uncertainty in the values extracted from the model eqs 2 and 3. The values of K_S were instead obtained from the graphs of Figure 6.

causes it to be flatter at long times. In contrast, if only the quantum yield Q were changing, then the curve under stress could be rescaled to look like the stress-free curve (see eq 2). In summary, the effect of the mechanical stress with the DNA spring in this particular position is complex: in terms of Michaelis–Menten parameters, the rates are sped up, but the quantum yield and the binding affinity for the substrate are reduced, while product inhibition is increased, so that overall luminescence is reduced. Thus, the integrated luminescence intensity of the chimera is a detector for the appearance of stress and therefore hybridization of the DNA spring.

It is interesting to compare these measurements with our previous results with guanylate kinase. GK has a known, large conformational change from the “open” to the “closed” structure upon binding the substrate GMP; therefore, it could perhaps be expected that pulling with the DNA spring against this conformational motion would affect substrate binding, which is correct. With the luciferase there is no such easy prediction, as this enzyme is a regularly shaped globule and substrate binding is not (at least not dramatically) of the induced fit kind. The fact that we are able, nonetheless, to modulate this enzyme’s activity with the DNA spring shows the generality of the principle that mechanically stressing an enzyme will affect activity, whether the enzyme has naturally

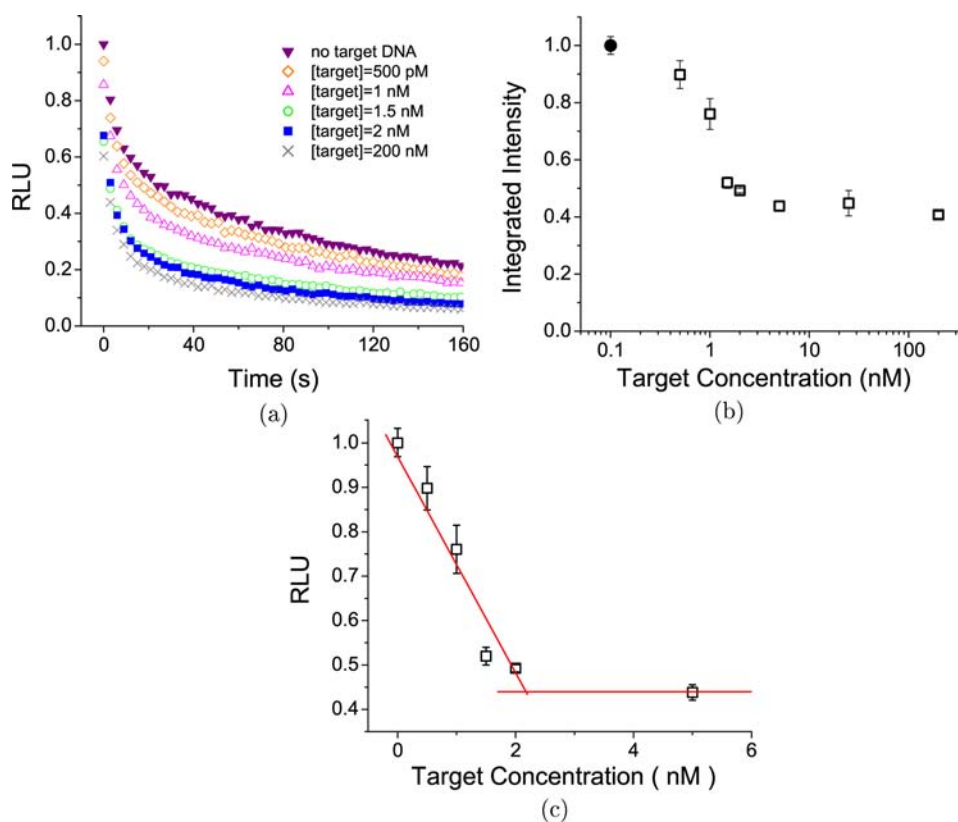


Figure 4. RLuc chimera as a molecular probe. Shown are results from a titration experiment where different amounts of target DNA (the 60mer complementary to the chimera DNA) are added to samples of the RLuc chimera; different amounts of target varying from 0.5 to 200 nM concentration in 40 μ L incubation volume were incubated overnight with the chimera at 2 nM concentration. To start the reaction, these samples were mixed with 160 μ L of substrate solution for a final substrate concentration of 1 μ M. (a) Time courses of the luminescence intensity for the ligated RLuc–DNA chimera mixed with different final concentrations of target 60mer, from 500 pM to 200 nM, in the 40- μ L incubation volume. (b) Integrated luminescence intensity (area under the curves in (a)) over 2 min for the chimera with different target concentrations, normalized by the intensity without target DNA. The solid circle represents the results without target DNA. (c) Same data as in (b) plotted on a linear concentration scale, showing that the integrated intensity decreases linearly with the concentration of target DNA until it saturates. Thus, the fraction of hybridized chimera is stoichiometric with the target in this regime of concentrations. The lines are linear fits for the linear decrease and saturated regions. The intersection provides a good estimate of the actual chimera concentration in the experiments.

occurring large conformational motion during the catalytic cycle.

Another interesting fact is that, in both cases (GK and RLuc), the forces we are able to apply with the DNA spring significantly reduce enzymatic activity but do not shut off the enzyme completely. Thus, at this level the mechanical response of these two very different structures is not entirely different.

The third interesting fact from comparing GK and RLuc is that, in both cases, there is a rather small effect ($\sim 20\%$ change or less) with the nicked DNA 60mer spring (in the case of GK, this effect, if present, is below the resolution of the measurements; for RLuc it is visible thanks to the higher resolution of the measurements); however, repairing the nick has a rather dramatic effect on the activity for both enzymes. We believe this behavior is due in essence to a nonlinearity of the mechanics of these systems, an issue which we explore in a forthcoming publication.

We now demonstrate the use of the luciferase–DNA chimera as a molecular probe. The target is the 60mer DNA sequence complementary to the chimera DNA; the RLuc–DNA chimera (in ligated, ss form) is the probe. Figure 4a shows the time course of luminescence measurements in a 40 μL sample volume containing approximately 2 nM RLuc–DNA chimera probe and varying amounts of the target oligo, reacting with 160 μL substrate solution so that the final substrate concentration is 1 μM . As the fraction of chimera hybridized to the target increases, luminescence decreases. The fraction of chimera hybridized is given, in this case, essentially by the stoichiometry, because the dissociation constant of this 60mer duplex is much smaller than 2 nM, the probe concentration in these measurements. This is shown in Figure 4c, where the luminescence signal (reported here as the area under the curves of Figure 4a) is seen to decrease linearly down to its asymptotic minimum value (see also Figure 4b). This minimum value is not zero because the DNA spring is not stiff enough to completely shut down the enzyme.²⁸ Since the dynamic range of this probe is roughly a factor 2 in light intensity (Figure 4), the detection limit in this particular format, in terms of amounts of target, is given essentially by the smallest amount of RLuc detectable with a signal/background of order 1, with the detector one is using. With our commercial luminometer, this is roughly 10 fmole. Of course, the concentration of the target must also be large enough that hybridization to the probe occurs.

We also tested the sensitivity of the RLuc–DNA probe in detecting mismatches in the target DNA. To this end, we used two 60 bp target strands carrying one and three (consecutive) mismatches at the center, respectively (oligomers 1MC and 3MC, see Experimental Section). Figure 5 shows that a single mismatch is easily detected by comparing the luminescence level with that of the chimera hybridized to the true complement. Several mismatches are even more easily detected. It is apparent that this probe has a peculiar sensitivity to localized defects in the DNA spring, which may release the mechanical tension. Here we show that this RLuc–DNA probe is capable of detecting a single-base mismatch at the center of a 60mer target DNA.

DISCUSSION

In this study, we demonstrate the concept of mechanical modulation of enzymatic activity on a molecule quite different in structure and function from the kinases used in previous work.^{17,29} The implication is that the DNA springs are a general

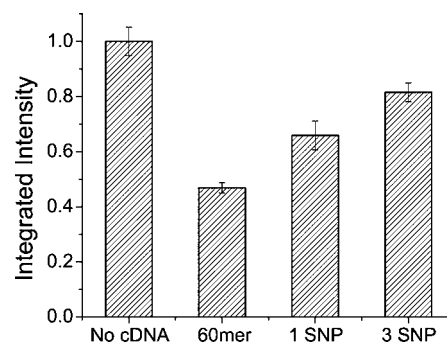


Figure 5. SNP detection with the RLuc chimera. We show the integrated luminescence intensity for the ligated chimera mixed with different targets. The results are normalized by the integrated intensity of the chimera alone (no target DNA). 1SNP and 3SNP represent the chimera hybridized with target 1MC and 3MC, having one mismatch and three consecutive mismatches in the center of the DNA spring, respectively. The conditions were the following: chimera concentration 2 nM and DNA target concentration 5 nM, incubation volume 40 μL . The figure shows that a single mismatch at the center of a 60mer target can be detected with this probe without the need to compare different temperatures.

method of control which can be applied to any enzyme, or at least to a variety of different enzymes. Now the functional response to mechanical stress¹⁸ can be studied for different enzymes with this method. In addition, the present construction using luciferase is particularly interesting because of the easy and sensitive measurement of enzymatic activity which requires only a small amount of enzyme. For example, this chimera is now a convenient tool to assess the relative bending stiffness of different DNA modifications and sequences.

The spring attachment points E161/S188 were chosen on the qualitative expectation that the stress applied at these locations would probably deform the substrate binding site and lead to an effect on the activity. While different sets of attachment points can evidently be explored experimentally,¹⁸ it would be useful to have theoretical predictions for “hotspots”³⁰ on the surface of the enzyme where an applied stress has a large effect, if such spots exist. Different approaches to this question have been proposed on the basis of phylogenetic analysis^{30–32} and MD simulations;^{8,33} we expect the dialogue between numeric analysis and experiments to intensify as more measurements with the enzyme–DNA chimeras become available.

The force the DNA spring exerts on the undeformed enzyme is known exactly in the case of the nicked spring, thanks to our independent measurements of the elastic energy of sharply bent DNA.^{34–36} We use the convenient formula given in eq 10 of Qu et al.³⁵ for the elastic energy $E(x)$ of the bent DNA, where x is the end-to-end distance (EED). The average force the DNA spring exerts on the undeformed enzyme is:

$$f = \left. \frac{\partial E}{\partial x} \right|_{x=s} = \left. \frac{\tau_c}{2R\sqrt{1 - \left(\frac{x}{2R}\right)^2}} \right|_{x=s} \quad (6)$$

where s is the distance between the Cys residues which defines the spring attachment points on the enzyme ($= 1.9$ nm) plus 2 times the length of the cross-linker ($= 2 \times 2.1$ nm), and we have used the upper form in eq 10 of Qu et al.³⁵ because the

DNA is kinked in this regime. Here, $R = L(1 - 2\gamma^2/45)$, $\gamma = L\tau_c/2B$, $2L = 0.33 \times N_d$ is the contour length of the DNA (N_d is the number of base pairs), $B = 200 \text{ pN} \times \text{nm}^2$ is the bending modulus and τ_c is the critical bending torque, a materials parameter which describes DNA elasticity in the kinked state.^{34–36} For the case where the DNA spring has a nick at the center, we have measured τ_c directly, and it is $\tau_c = 27 \text{ pN} \times \text{nm}$,^{34,35} essentially independent of the sequence.³⁶ Thus, using the parameters for the present case, namely $2L = 20 \text{ nm}$ and $s = 6.1 \text{ nm}$, we find from eq 6 that the force on the enzyme is $f = 1.5 \text{ pN}$. Note that, taking the worm-like-chain (WLC) expression for the elastic energy of the DNA (i.e., if the DNA was not kinked) gives $f = 5 \text{ pN}$, significantly overestimating the force. In conclusion, we are able to assign a precise value to the force which causes the small but measurable modulation of enzymatic activity seen in Figure 2a, namely, $f = 1.5 \text{ pN}$. The force for the non-nicked case is more delicate and needs a longer discussion which we will provide elsewhere.

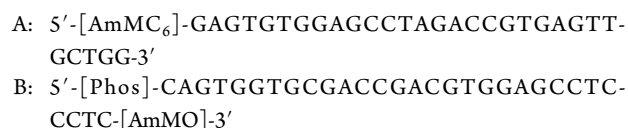
We believe quantitative measurements such as those presented here may prove quite useful in validating future MD simulations addressing mechano–chemical coupling in enzymes, while experimentally we feel our results may open a Pandora’s box of studies of mechano–chemical coupling with a variety of enzymes. Theoretical insights about mechano–chemical couplings can now be tested on a variety of enzymes! For instance, the present observation that stressing this enzyme has the opposite effect on binding of the substrate and the product (substrate binding affinity is decreased, product binding affinity is increased, see Table 1) is probably a nice example of the concept of “conformational proofreading” introduced by Savir and Tlusty.³⁷

Finally, we demonstrate the RLuc–DNA chimera as a molecular probe for the detection of specific DNA sequences. RLuc and other luciferases are, of course, commonly used as bioluminescent reporters in studies of gene expression and regulation. The advantages of using a luciferase reporter gene are that bioluminescence is typically not endogenous to the cell of interest and the corresponding assay is sensitive, quantitative, and easy. A molecular probe based on luciferase retains these advantages, and the present construction represents one such probe. It is not our purpose here to present a detailed comparison with other DNA detection assays; we merely mention that other homogeneous assays, such as the molecular beacons^{38–40} and the enzyme–DNA–inhibitor probe of Saghatelian et al.⁴ are not bioluminescence based, while other sensitive detection schemes such as cyclic voltammetry,⁴¹ scanometric DNA array,⁴² and electrochemical DNA sensors^{43–45} are surface bound. Regarding SNP detection, for existing assays the hybridized sequence is shorter than 20 bp, whereas our longer 60 bp construct presumably should translate to the ability of detecting mismatches at very low target concentrations. Ours is also, we believe, the only homogeneous assay where SNP detection is achieved without some form of melting curve analysis.

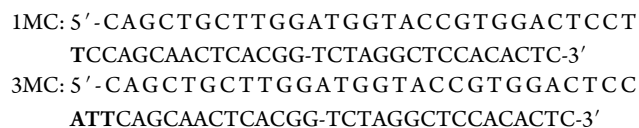
Future work may address the question of whether the present probe or derivations thereof can be useful for in vivo detection inside the cell and whether incorporating aptamers in the DNA spring^{46–48} can lead to the design of a more general small-molecules detector.

EXPERIMENTAL SECTION

DNA and Cross-Linker. The synthetic DNA oligonucleotides were purchased from Integrated DNA Technology (IDT). The sequences of the two DNA 30mer arms with which the chimera was constructed were:



where [AmMC₆] and [AmMO] were amino terminal modifications at the 5′ and 3′ ends, respectively. [Phos] is the phosphate modification, enabling to subsequently link the two DNA arms by ligation. RA and RB were the complementary DNA of A and B arm, respectively. The amino-functionalized DNA strand was attached to the Cys residues through a heterobifunctional cross-linker (NHS-PEO2-maleimide), which reacts with the amine group on the DNA via the NHS to form an amide bond and the sulfhydryl group of the Cys via the maleimide group to form a stable thioether bond. The 60 bp DNA complementary to A plus B was: 60mer: 5′-CAGCTGCTTGGATGGTACCGTGGACTCCTCCTGCCAGCAACTCACGGTCTAGGCTCCACTC-3′ and was used to obtain the ds chimera. We also designed two 60 bp DNA oligomers having one and three mismatches relative to the chimera DNA; the sequences were:



The bold letters represent the mismatched nucleotides.

Mutagenesis and Protein Purification. The wild-type gene of Renilla luciferase (RLuc) was obtained from vector pRL-null (Promega) and subcloned to vector pET28a (Novagen) with a His-tag at the C-terminal to facilitate the purification after protein expression. To construct the mutant, the wild-type gene was modified by site-directed mutagenesis to substitute two cysteins at residues 161 and 188 for later DNA conjugation. The mutant proteins were expressed in *E. coli* strain BL21(DE3)pLysS and induced with 1 mM IPTG for 3 h at 30 °C.²⁷ The product proteins were purified by Ni-NTA chromatography (Qiagen) through the His-tag. Because of a tendency for this protein to self-associate, the concentration of RLuc is kept under 25 μM , and we generally avoid vortexing and centrifugation of the samples.

Protein–DNA Complex Synthesis. The synthesis of RLuc–DNA two-armed chimera is adapted and optimized from the method described in ref 19. The two DNA arms are attached sequentially using HPLC purification of the intermediate products. First, luciferase is mixed with DNA arm A in the molar ratio 9:1 in 100 mM sodium phosphate, 1 mM EDTA, and 150 mM sodium chloride buffer at room temperature (approximate protein concentration is 20 μM).

After 90 min of incubation, the mixture is passed through an ion-exchange chromatography column (HPLC: Bio-Rad) to separate the one-armed chimera from other species. DNA arm B is then added to the one-armed chimera (approximate concentrations 0.5 μM), and the mixture is incubated overnight at 4 °C. The final synthesized two-armed chimera was purified by Ni-NTA chromatography through the His-tag on the protein and verified by the corresponding molecular weight on sodium dodecyl sulfate polyacrylamide gel electrophoresis (SDS-PAGE, Bio-Rad).

Determination of Enzyme Concentration. Protein concentration is measured with the Bradford assay (Bio-Rad) or, for small quantities, from the intensity of the bands on SDS-PAGE images, where proteins are stained with SYPRO Ruby Protein Gel Stain (Invitrogen). From the result of the cDNA detection experiment, it turns out that using the titration of cDNA and finding the minimum

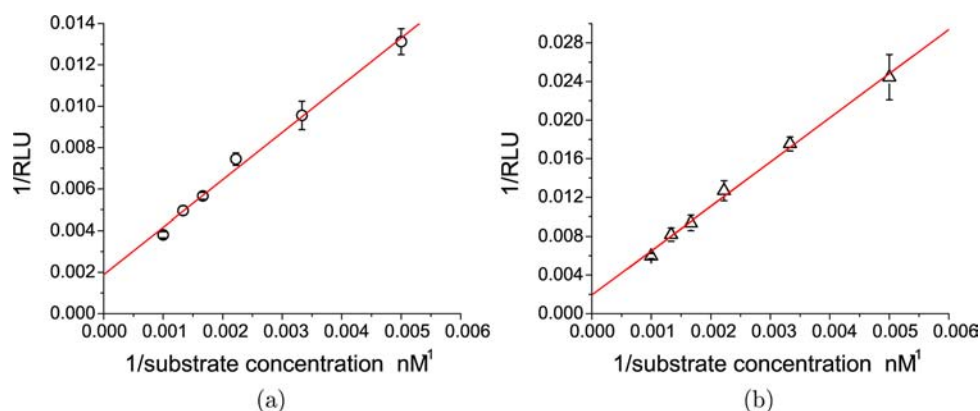


Figure 6. Determination of K_S for ss chimera and ds 60mer using double reciprocal plot: reciprocal of reaction rate vs reciprocal of substrate concentration. The slope divided by the intercept is K_S .

concentration which saturates the effect of reducing luminescence is a more precise way to determine chimera concentration. (Figure 4c)

Ligation. We employed T4 DNA ligase (New England Biolab) to link the A and B arms of the chimera. The sample is incubated for two days at 16 °C under the following conditions: 20 nM chimera, 1.25 μ M 18mer cDNA, which serves as splint to hold the two free ends of the DNA arms, 0.1 mg/mL of BSA (New England Biolab), and 1.2 units/ μ L of ligase in the recommended reaction buffer. After ligation, Ni-NTA purification is performed to remove the DNA splint, ligase, and ATP. Products of the ligation reaction are identified by gel electrophoresis; the yield of correct construction (ligated chimera) was more than 75%.

Kinetics of Enzyme Activity. RLuc–DNA chimera was incubated with or without target DNA at room temperature overnight in PBS (pH 7.4) with 0.4 mg/mL BSA. In the mixture, the chimera concentration was between 1 to 6 nM, while the target DNA concentration was 60 times the chimera concentration unless otherwise specified. The stock concentration of Coelenterazine-h substrate (Promega) was 50 μ M in methanol. The substrate solution was further diluted in PBS (pH 7.4) right before the luminescence measurements. Due to the fast inactivation of RLuc, the microplate was modified to allow the substrate solution to be manually injected to mix with the chimera sample and initiate the luminescence, enabling to monitor the beginning of the reaction with our commercial microplate reader (Synergy HT, BioTech) For each measurement, 160 μ M substrate solution was added to 40 μ L sample.

Fitting of Experimental Data. Luminescence measurements were performed with many different substrate concentrations, from 200 to 1000 nM, but we particularly fitted the data with concentrations of 600, 750, and 1000 nM. Because there are many parameters (see eqs 2 and 3), we employed the following strategy. First, we calculated K_S by using a double reciprocal plot: reciprocal of reaction rate vs reciprocal of substrate concentration. Since the molar ratio of substrate to enzyme is large (>500), in the beginning of the reaction, the substrate concentration can be approximated as a constant and $[P]/[S]$ is approaching zero. Taking the reciprocal of eq 2 gives

$$\frac{1}{\frac{d}{dt}N_\gamma} = \frac{1}{[E]k_{\text{cat}}VQ} \left(1 + \frac{K_S}{[S]} \right) \quad (7)$$

We therefore plot $1/(\text{luminescence signal})$ vs $1/[S]_0$ (the initial substrate concentration), fit a straight line, and obtain K_S as the slope over the intercept (Figure 6). We took the first (“zero time”) data point of each reaction as the reaction rate for that specific initial substrate concentration, analyzed all the data for different substrate concentrations (Figure 6), and calculated K_S for the ss chimera and the ds chimera (Table 1).

Next, we write the measured luminescence intensity I as:

$$I(t) = A \frac{dN_\gamma}{dt} \quad (8)$$

where A is an instrument-dependent numerical factor (the conversion factor between rate of emitting photons and luminometer reading). From eq 5:

$$\frac{d}{dt}N_\gamma = VQ \frac{d[S]}{dt} \quad (9)$$

$$\Rightarrow I(t) = BV \frac{d[S]}{dt} \quad \text{where } B = AQ \quad (10)$$

The equations which evolve the quantities $[S]$, $[E]$, and $[P]$ are (see eqs 2–5)

$$\begin{aligned} \frac{d[S]}{dt} &= -\frac{[E]k_{\text{cat}}}{1 + \frac{K_S}{[S]} + \frac{K_S[P]}{K_P[S]}} \\ \frac{d[E]}{dt} &= \frac{k_d}{k_{\text{cat}}} \frac{d[S]}{dt} \\ \frac{d[P]}{dt} &= -\frac{d[S]}{dt} \end{aligned} \quad (11)$$

while the intensity at time zero is

$$I(0) = I_0 = B \frac{[E]_0 k_{\text{cat}} V}{1 + \frac{K_S}{[S]_0}} \quad (12)$$

We fit the three parameters k_{cat} , k_d , and K_P as follows. Starting from the known initial values $[S]_0$, $[E]_0$, $[P]_0 = 0$, and K_S determined above, and choosing values for k_{cat} , k_d , and K_P , we evolve eq 11 in time. B is determined from the luminescence at zero time I_0 using eq 12. Then the luminescence intensity in the course of time, $I(t)$, is determined from eq 10. This is compared to the experimental curve and the parameters k_{cat} , k_d , and K_P are varied to minimize the square difference (least-squares fit). The procedure returns values for k_{cat} , k_d , K_P , and the parameter B which is proportional to the quantum yield Q (see eq 10). In this way, we generated the reaction curves numerically and fit the luminescence measurement with substrate concentrations of 600, 750, and 1000 nM by adjusting k_d , k_{cat} , and K_P . The best-fit set of values of k_d , k_{cat} , and K_P for each construction is reported in Table 1. We also report the value of B , since the ratio of the B values with and without stress is equal to the ratio of the corresponding Q values (the instrumental parameter A being the same for all experiments).

Sensitivity in Detecting the Target DNA. Luminescence measurements were conducted for ligated RLuc–DNA chimera mixed with different concentrations of DNA 60mer, from 500 pM to 1 μ M. The estimated chimera concentration was 2 nM (see Determination of Concentration section). The luminescence intensities were integrated over 2 min and normalized by the integrated luminescence of the ligated, unhybridized RLuc–DNA chimera sample.

Detection of Mismatches in Target DNA. RLuc–DNA chimera was incubated alone or with different target DNA, including 60mer, 1MC, and 3MC, in PBS (pH = 7.4) with 0.4 mg/mL BSA. The concentrations of chimera and DNA were 2 nM and 5 nM, respectively. The luminescence measurements were conducted as described in the Kinetics of Enzyme Activity section.

AUTHOR INFORMATION

Corresponding Author

tseng@physics.ucla.edu (C.-Y.T.); zocchi@physics.ucla.edu (G.Z.).

Notes

The authors declare no competing financial interest.

ACKNOWLEDGMENTS

We thank the Arbin group at UCLA for the use of the Protein Expression Lab facilities. This work was supported by NSF grant DMR-1006162, and by the US-Israel Binational Science Foundation under Grant Number 2010448.

REFERENCES

- Zocchi, G. *Annual Rev. Biophys.* **2009**, *38*, 75–88.
- Koshland, D. E. *Angew. Chem., Int. Ed. Engl.* **1995**, *33*, 2375–2378.
- Choi, B.; Zocchi, G.; Canale, S.; Wu, Y.; Chan, S.; Perry, L. J. *Phys. Rev. Lett.* **2005**, *94*, 038103.
- Saghatelian, A.; Guckian, K. M.; Thayer, D. A.; Ghadiri, M. R. *J. Am. Chem. Soc.* **2002**, *125*, 344–345.
- Miduturu, C. V.; Silverman, S. K. *J. Am. Chem. Soc.* **2005**, *127*, 10144–10145.
- Zelin, E.; Silverman, S. K. *ChemBioChem* **2007**, *8*, 1907–1911.
- Zelin, E.; Silverman, S. K. *Chem. Commun.* **2009**, *0*, 767–769.
- Sacquin-Mora, S.; Delalande, O.; Baaden, M. *Biophys. J.* **2010**, *99*, 3412–3419.
- Perutz, M. F. *Nature* **1972**, *237*, 495–499.
- Hopfield, J. J. *J. Mol. Biol.* **1973**, *77*, 207–222.
- Mayans, O.; van der Ven, P. F. M.; Wilm, M.; Mues, A.; Young, P.; Furst, D. O.; Wilmanns, M.; Gautel, M. *Nature* **1998**, *395*, 863–869, DOI: 10.1038/27603.
- Puchner, E. M.; Alexandrovich, A.; Kho, A. L.; Hensen, U.; Schäfer, L. V.; Brandmeier, B.; Gräter, F.; Grubmüller, H.; Gaub, H. E.; Gautel, M. *Proc. Natl. Acad. Sci. U.S.A.* **2008**, *105*, 13385–13390.
- von Castelmur, E.; Strümpfer, J.; Franke, B.; Bogomolovas, J.; Barbieri, S.; Qadota, H.; Konarev, P. V.; Svergun, D. I.; Labeit, S.; Benian, G. M.; Schulten, K.; Mayans, O. *Proc. Natl. Acad. Sci. U.S.A.* **2012**, *109*, 13608–13613.
- Pfuhl, M.; Gautel, M. *J. Muscle Res. Cell Motil.* **2012**, *33*, 83–94.
- Sekulic, N.; Shuvalova, L.; Spangenberg, O.; Konrad, M.; Lavie, A. *J. Biol. Chem.* **2002**, *277*, 30236–30243.
- Blaszczak, J.; Li, Y.; Yan, H.; Ji, X. *J. Mol. Biol.* **2001**, *307*, 247–257.
- Choi, B.; Zocchi, G. *Biophys. J.* **2007**, *92*, 1651–1658.
- Tseng, C.-Y.; Wang, A.; Zocchi, G. *Europhys. Lett.* **2010**, *91*, 18005.
- Wang, Y.; Wang, A.; Qu, H.; Zocchi, G. *J. Phys.: Condens. Matter* **2009**, *21*, 335103.
- Matthews, J. C.; Hori, K.; Cormier, M. J. *Biochemistry* **1977**, *16*, 85–91.
- Loening, A. M.; Fenn, T. D.; Wu, A. M.; Gambhir, S. S. *Protein Eng. Des. Sel.* **2006**, *19*, 391–400.
- Ward, W. W.; Cormier, M. J. *J. Biol. Chem.* **1979**, *254*, 781–788.
- Wang, Y.; Wang, G.; O’Kane, D.; Szalay, A. *Biolumin. Chemilumin.: Mol. Rep. Photons* **1997**, 419–422.
- Xu, Y.; Piston, D. W.; Johnson, C. H. *Proc. Natl. Acad. Sci. U.S.A.* **1999**, *96*, 151–156.
- Loening, A. M.; Fenn, T. D.; Gambhir, S. S. *J. Mol. Biol.* **2007**, *374*, 1017–1028.
- Matthews, J. C.; Hori, K.; Cormier, M. J. *Biochemistry* **1977**, *16*, 5217–5220.
- Woo, J.; von Arnim, A. *Plant Methods* **2008**, *4*, 23.
- Tseng, C.-Y.; Wang, A.; Zocchi, G.; Rolih, B.; Levine, A. J. *Phys. Rev. E* **2009**, *80*, 061912.
- Choi, B.; Zocchi, G. *J. Am. Chem. Soc.* **2006**, *128*, 8541–8548.
- Lockless, S. W.; Ranganathan, R. *Science* **1999**, *286*, 295–299.
- Lee, J.; Natarajan, M.; Nashine, V. C.; Socolich, M.; Vo, T.; Russ, W. P.; Benkovic, S. J.; Ranganathan, R. *Science* **2008**, *322*, 438–442.
- Halabi, N.; Rivoire, O.; Leibler, S.; Ranganathan, R. *Cell* **2009**, *138*, 774–786.
- Delalande, O.; Sacquin-Mora, S.; Baaden, M. *Biophys. J.* **2011**, *101*, 1440–1449.
- Qu, H.; Tseng, C.-Y.; Wang, Y.; Levine, A. J.; Zocchi, G. *Europhys. Lett.* **2010**, *90*, 18003.
- Qu, H.; Zocchi, G. *Europhys. Lett.* **2011**, *94*, 18003.
- Sanchez, D. S.; Qu, H.; Bulla, D.; Zocchi, G. *Phys. Rev. E* **2013**, *87*, 022710.
- Savir, Y.; Tlusty, T. *PLoS One* **2007**, *2*, e468.
- Tyagi, S.; Kramer, F. R. *Nat. Biotechnol.* **1996**, *14*, 303–308.
- Nutiu, R.; Li, Y. *Nucleic Acids Res.* **2002**, *30*, e94.
- Grossmann, T.; Röglin, L.; Seitz, O. *Angew. Chem., Int. Ed.* **2007**, *46*, 5223–5225.
- Fan, C.; Plaxco, K. W.; Heeger, A. J. *Proc. Natl. Acad. Sci. U.S.A.* **2003**, *100*, 9134–9137.
- Taton, T. A.; Mirkin, C. A.; Letsinger, R. L. *Science* **2000**, *289*, 1757–1760.
- Kelley, S. O.; Boon, E. M.; Barton, J. K.; Jackson, N. M.; Hill, M. G. *Nucleic Acids Res.* **1999**, *27*, 4830–4837.
- Xiao, Y.; Lou, X.; Uzawa, T.; Plakos, K. J. I.; Plaxco, K. W.; Soh, H. T. *J. Am. Chem. Soc.* **2009**, *131*, 15311–15316.
- Drummond, T. G.; Hill, M. G.; Barton, J. K. *Nat. Biotechnol.* **2003**, *21*, 1192–1199.
- Farokhzad, O. C.; Cheng, J.; Teply, B. A.; Sherifi, I.; Jon, S.; Kantoff, P. W.; Richie, J. P.; Langer, R. *Proc. Natl. Acad. Sci. U.S.A.* **2006**, *103*, 6315–6320.
- Swensen, J. S.; Xiao, Y.; Ferguson, B. S.; Lubin, A. A.; Lai, R. Y.; Heeger, A. J.; Plaxco, K. W.; Soh, H. T. *J. Am. Chem. Soc.* **2009**, *131*, 4262–4266.
- McKeague, M.; DeRosa, M. C. *J. Nucleic Acids* **2012**, *2012*, 20.